Instituto Nacional de Astrofísica, Optica y Electrónica.

REPORTE TÉCNICO
No. 631

COORDINACION DE ASTROFISICA

Atmospheric water vapor content estimations based on Meteorological Radiosounding Data

Mendoza-Torres José-Eduardo

Atmospheric water vapor content estimations based on Meteorological Radiosounding Data

Abstract

Radiosounding data are used to estimate the atmospheric water vapor content, starting from the meteorological parameters (Temperature, Pressure and Relative Humidity) measured by the sonde at different altitudes. Data taken at Mexico City are used as example. The number density of H_2O is estimated at the altitudes where the radiosonde takes data. It is found that, for December, January and February, the scale height of water vapor content takes the highest values of the year. The Precipitable Water Vapor (PWV) is estimated by integrating the density of water vapor molecules from various lower limits. Histograms of the PWV values obtained for the lower limits of integration have been also made. For summer time the histograms of the PWV have a maximum that takes place at 35 mm for 2.0 km and shifts to lower values as the lower limit of integration increases. For winter time, the histograms for low lower limits of integration do not have a prominent maximum but are considerably spread. However, for the PWV integrated from the highest low limits of integration the Histograms have a well defined maximum and the shape of the distributions is rather sharp. In winter time at Mexico City, which is a mid-altitude site, the PWV takes values as low as those observed at 5-6 km altitude.

Introduction

The Water Vapor Content at the atmosphere depends on many factors, as flows in a variety of directions, convective motions at different altitudes, time-variable local conditions and water masses and flows on the Earth surface. This makes the Water Vapor Content to be highly variable with geographic coordinates and at different time scales.

The importance of the atmospheric water in the climate, and in general in the Earth life, makes it the subject of study in a variety of Sciences, including, Astronomy (Otárola et al., 2009), Earth Sciences as Meteorology, Geophysics (Vogelmann et al., 2008), and other, and also for services as the Weather Forecasting. For all of them, the study of the Water Vapor Content is important, particularly in the last years with the global climate change, which is leading, in one hand, to considerably stronger precipitations, and even floods at several locations, and to the lack of water and even droughts at other sites. The water content is important not only because the importance of water flows and precipitations but also because possibly, it could play a main role in the Green-House effect.

The water content at a given site is usually expressed by using a single value which is the amount of Precipitable Water Vapor (PWV), as we will see below. The opacity of the atmosphere is very dependent on the PWV. Even at high altitude astronomical observatories (as the Sierra Negra Volcano, whose summit is at 4500 m.s.n.m.) the periods with high values of PWV are not favorable for observations. Then, a better knowledge of the behavior of PWV with time is important for astronomical observations, in particular at millimeter and infrared wavelengths, where the atmospheric opacity is large.

A linear relation has been found between PWV and the opacity at various wavelengths, as 1.4 mm (Otárola et al., 2009) and 1.6 mm (Delgado 1999) giving quantitative information of the quality of the sky for Astronomical observations at these wavelengths. Therefore, the studies and monitoring of PWV at particular sites (Hills and Richer, 2000) could allow observers to identify the time periods when it has the lowest values, making the site more feasible for observations and even giving the possibility to improve the planning of observations based on the PWV forecasting (Pérez-Jórdan et al., 2015).

The PWV can be estimated by several ways, including some with the use of GPS (Tregoning et al. 1998), with observations from space at near and mid infrared wavelengths, 0.4-14 μm (King et al. 2003), 20 μm (Naylor et al., 2002), 6.5 μm and 10.7 μm (Marín et al., 2015), at far IR wavelengths (also considered submillimeter wavelengths), for example, 850 and 450 μm (Holland et al., 1999) and 350 μm (Radford et al. 1998), ground based radiometric observations at frequencies around the 22.2-GHz H_2O emission line (Turner et al. 2007) or near the H_2O line at 183 GHz (Hills and J. Richer, 2000 and Pozo et al. 2016). In this work, radiosounding data are used to estimate de PWV.

Variation of Water Vapor Content with Altitude

The number density of a given molecular species varies with height *N(h)* at the atmosphere. In Figure 1 an example of the H_2O number density as function of altitude is shown. The black continuous line was obtained by a differential absorption method using laser pulses with on-and-off observations of an H_2O IR absorption line (Vogelmann et al., 2008**)**. The red circles were obtained with radiosonde at balloons, which provide meteorological parameters with altitude. It may be seen that the density of H_2O molecules shows a trend with altitude (a general decay) and that most of the content of H_2O is concentrated below an altitude of about 9 km (Figure 1). Above this altitude, the content of H_2O is very low,

particularly in comparison with the PWV at the sea level and few kilometers above it.

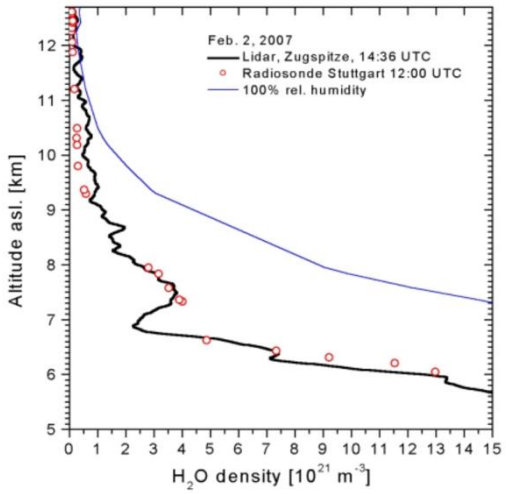

Figure 1. Density of H_2O molecules at the atmosphere as a function of altitude, based on observations of an H_2O infrared absorption line with an on-and-off method (continuous lines) and with meteorological sondes (circles) (taken from Vogelmann and Trickl, 2008).

Some methods to estimate the water content are based on integrated parameters through the atmosphere or along part of it, as Satellite images, radiometers on Earth and GPS. Most of them cannot give an altitude profile as that of Figure 1. On the other hand, radiosondes provide in-situ measurements, that allow to estimate the water vapor density at a series of altitudes.

The scale height of the water vapor density

The general trend of the number density *N(h)* of a given molecular species may be approximated by a simple function and may be estimated under given conditions. In the case of hydrostatic equilibrium, it can be expressed with an exponential function, as follows,

$$N(h) = N_0 \, e^{-\frac{h}{H}} \qquad (1)$$

where h is the altitude, N_0 is the number density for a reference altitude and H is the scale height for the density of the given species. Due to the complex variations of the water content at the atmosphere, strictly speaking, it is not at hydrostatic equilibrium and the actual H_2O density altitude has deviations from a smooth trend (as those seen in Figure 1). Nevertheless, a scale height H may be used to describe the number density of H_2O in a general way, by using an exponential function (Giovanelli et al. 2001).

From Equation 1 we may see that, when the altitude equals the scale height, $h=H$, the density is $N = \frac{N_0}{e}$ ($N \approx \frac{1}{3} N_0$). Then, for a given density N_0 (at the reference altitude), as larger is H as higher will be the altitude where the density will reach the value $\frac{N_0}{e}$. It means, with the increase of H, the H_2O content would decrease more slowly with altitude. For $H \to \infty$, the density would be $N \to N_0$. In that case, the density would tend to be constant and, in an altitude profile as that of Figure 1, the density profile will tend to be vertical. In a more general case, as above mentioned, for a given moderate large H, the density decreases less with altitude than for a smaller H.

Radiosounding Data

At a given altitude, the temperature (T), pressure (P) and relative humidity (RH) are measured with Meteorological Radiosondes. As we will see below, using these data, the number density of H_2O molecules, at each altitude, may be estimated and then, the integrated content of H_2O at the atmosphere, computed. The result of the integration or PWV is in fact the water vapor content in a vertical column of the atmosphere.

For a given altitude h, the dew point temperature $T_d(h)$ may be estimated with the relative humidity $RH(h)$ and the temperature $T(h)$ (Lawrence, 2005) as follows

$$T_d(h) = T(h) - ((100 - RH(h))/5) \qquad (2)$$

where the variables are function of the altitude.

Based on the temperature of the dew point (T_d), the water vapor pressure (P_s) may be estimated, for example, by using the formula derived by Alduchov and Eskridge (1996),

$$P_s = 6.1094 \exp\left(\frac{17.625\, T_d}{T_d + 243.04}\right) \qquad (3)$$

where P_s corresponds to a given altitude, it is given in hPa and T_d in *degrees Celcius*. Using $P_s(h)$ and the local temperature at the altitude h, we can estimate the number density of water vapor molecules $n_w(h)$ at that given altitude with the assumption that the ideal-gas-law holds

$$n_w(h) = \frac{P_s(h)}{kT(h)} \qquad (4)$$

The volume density of water vapor molecules at a given altitude ($\rho(h)$) is

just the product of the number density $n_w(h)$ and the mass of a water molecule, which is 18 amu = 2.99×10^{-23} g. The mass *M* of a column of water vapor between two different altitudes can be estimated by using the average of *ρ(h)* between the two given altitudes. The difference between these altitudes may be considered the length of the column for the average volume density. The volume of this column is given by the product of this length and the base of the column (which we consider 1 cm^2). Then, the mass of waver vapor in such a column is obtained just by multiplying the volume of the column and the average volume density between the given two altitudes. The total column is obtained by integrating (or summing) over all the altitudes

The mass obtained for a column of water vapor is compared with a column of liquid water (whose base is also of 1 cm^2). Then, using the density for liquid water ($1\ g/cm^3$), the altitude of the column of equivalent liquid water is computed. Precisely, the height of this last column (of liquid water) is the parameter used to describe the integrated water vapor, that is referred to as Precipitable Water Vapor (PWV) and it is given in *mm*. It is convenient to pay attention to this fact, and further remember that the PWV corresponds to the height of the equivalent column of liquid water.

Data

Let's recall that the PWV is estimated by integrating the water vapor content at the range of altitudes where the meteorological radiosondes take data. They are limited, on the low altitudes by the site where the balloon is released and, on the other extreme, by the altitude where the radiosonde sends the last measurements, which typically occurs higher than 10 *km*.

Meteorological radiosondes are released in Mexico City two times a day, at noon and at midnight. In this work data taken from 1973 to 2015, at noon, are analyzed. The altitude of Mexico City is 2.2 km, and consequently the data are taken from altitudes above this one. Nevertheless, it is possible to extrapolate the values obtained to estimate the PWV, as if it would be integrated from 2.0 km. In such a way the computations of PWV have been made for a series of lower altitudes (the lower in the sense that each of them corresponds to a lower limit of integration), which are: 2.0, 2.5, 3.0, 3.5, 4.0, 4.5, 5.0, 5.5 and 6.0 km. The higher limit of integration, as above mentioned, is larger than 10 km in most of the cases.

Results

In Figure 2 we may see the values of PWV for the 2012 year. The different colors of the data points are for the PWV integrated from different lower altitudes (as indicated in the figure). It may be seen that the PWV integrated from 6 km (data in red) takes the lowest values. This is expected since, as above mentioned, the H_2O content is low above ~ 9 k. It means, the integration from 6 km, includes a short altitude interval with large content of H_2O. The PWV obtained from lower altitudes of integration takes larger values, being the largest one for the 2 km lower limit of integration. From Figure 2, it may be seen that the PWV is low at the beginning of the year, grows to the middle (summer) and again decreases to the end. In Figure 3 the PWV integrated from 2.0 km (red), 3.5 km (blue) and 6.0 km (violet) lower altitudes is shown. The periodic variations correspond to changes over a year. In Figure 4 the PWV is shown for the whole period analyzed (1973-2015). Further some other aspects of the behavior of PWV are shown based on Figures 5 to 15.

In Figure 5 the monthly averages of PWV for December of each year are given, with bars are indicated the standard deviations. In the PWV integrated from 2 km (black line) a decrease is seen during 1999-2004. In Figures 6 and 7 also the average by month of PWV are shown, the decrease at 1999-2004 is also seen. In the PWV integrated from 2 km, the decrease is more evident for November and December data (Figure 7). At the PWV integrated from 3 km the decrease is also seen, but it is deeper at the 2 km one. This indicates that during the winter of these years, the average of the H_2O content decreased at low attitudes respect the previous years. As may be seen from Figure 8, in this period, there are more values with smaller PWV than during other years. Also, at 1978-1980 and at 2009-2013, a similar situation, although less pronounced, is observed. Such behavior could probably be a result of the global climate change.

We may see in Figures 9 and 10 that from October to March (let's say Winter Months) the PWV is smaller than for the rest of the year (say Summer Months). The difference between PWV at Winter Months respect Summer Months is largest for the PWV integrated from 2 km. The difference decreases with the altitude of the lower limit of integration and it is smaller for the PWV integrated from 6 km. Also, it may be seen that the PWV for October has similar values to those of May. In particular the PWV from 2 km for May is larger than for October, but at 3 km the values are very similar to each other. For 3.5 km, and larger altitudes, the PWV for May is slightly lower than for October. This means that in May the content of water vapor is larger only integrated

from $h<3$ km respect that for October. It means, for October, the PWV decreases less with the altitude (of the lower limit of integration). On the other hand, the less the PWV decreases with this altitude, the larger the scale height is. Then, for October, the scale height is larger than for May. From Figure 10, we may see that for December, January and February, the scale height takes the highest values of the year.

The histograms for the PWV integrated from 6 km (Figures 11 and 12) for August and September have a maximum at about 35 mm. The histogram predominantly has values around this maximum and the frequency of occurrence smoothly decreases to both sides. The histogram of the PWV, integrated from 2.5 km, has a maximum at 23-25 mm. At the histograms for the subsequent altitudes (higher altitudes of the lower limit of integration) the maximum shifts to lower values of PWV.

From Figures 13 and 14, it may be seen that the histograms of the PWV integrated from 2km for December and January do not have a prominent maximum but the values are extended over a wide range. The values of PWV integrated from 2 km are considerably more spread in December and January than in August and September showing that, some values of the PWV in winter time are as high as the PWV in summer at the same altitude. However, it may be seen that for some periods, also at 2 km, the PWV in winter is as low as the PWV for 6 km. In particular, as may be seen from Figure 13, in January, there are more low values of PWV at 2 km than in December. In fact, January has the lowest PWV values at the year. Even, during some time intervals, the PWV from 2 km could be, for Astronomical observations, as good as from 6 km.

The histogram of PWV values of all the months for a 2 km lower limit (Figures 15 and 16) does not have a prominent maximum. The frequency of occurrence is almost the same for PWV from 3 mm to about 40 mm, leading to an extended distribution with a flat top. For 2.5 km the histogram is also extended but shorter than for 2.0 km (flat from about 3 mm to 30 mm) but with a higher frequency of occurrence in this range. As going to lower altitudes of integration (3.0 km and larger), the maximum of the histogram becomes more prominent and the frequency of occurrence becomes larger, for values closer to this maximum. Then, the histogram becomes thinner as the lower altitude of integration increases. For the 6 km lower altitude, the histogram has a very prominent maximum with a frequency of occurrence of more than 1700 cases for a PWV of about 0.5 mm and the bulk of PWV data lies in values smaller than 5 mm. These results indicate that for an altitude of 6 km, the PWV is predominantly low and, consequently, the histogram has

a sharp shape. It means, as integrating from lower altitudes, the PWV values spread over larger and larger ranges. This makes the histogram of 2 km to be the most extended of all. This altitude corresponds to the lower limit of integration of the present study and therefore to the longest path through the atmosphere.

Conclusions

Data obtained by meteorological radio sounding are used to study the behavior of the water vapor content with time and altitude. Variations of the PWV at time scales of various years as well as of shorter periods are identified. It is found that for summer time the histograms of the PWV have a clear maximum that shifts to lower values as the lower limit of integration increases. It is seen that from December to February, the scale height of the H_2O content takes the largest values. For winter time, the histogram for PWV at low altitudes does not have a prominent maximum and the histograms are considerably more spread than in summer. The behavior of the histograms indicates that, at winter, the PWV at 2 km could be as good as at 6 km for Astronomical observations. Nevertheless, for an altitude of 6 km, the PWV is predominantly low. Also, a minimum in the water vapor content at altitudes of 2-3 km is seen during 1999-2004, in particular during winter, which probably could be a result of the global climate change

References

Giovanelli, Riccardo; Darling, Jeremy; Henderson, Charles; Hoffman, William; Barry, Don; Cordes, James; Eikenberry, Stephen; Gull, George; Keller, Luke; Smith, J. D.; Stacey, Gordon, Publications of the Astronomical Society of the Pacific, Volume 113, Issue 785, pp. 803-813, 2001

Lawrence, Mark G., 2005: The relationship between relative humidity and the dewpoint temperature in moist air: A simple conversion and applications. Bull. Amer. Meteor. Soc., 86, 225-233. doi: http;//dx.doi.org/10.1175/BAMS-86-2-225

Alduchov, Oleg; Eskridge, Robert, Improved Magnus Form Approximation of Saturation Vapor Pressure, Journal of Applied Meteorology, vol. 35, Issue 4, pp.601-609, 1996

R. Hills and J. Richer, "ALMA Memo 303: Water vapor radiometers for ALMA", http://library.nrao.edu/public/memos/alma/memo303.pdf, 2000

W.S. Holland, E.I. Robson, W.K. Gear, C.R. Cunningham, J.F. Lightfoot, T. Jenness, R.J. Ivison, J.A. Stevens, P.A.R. Ade, M.J. Griffin, W.D. Duncan, J.A. Murphy and D.A. Naylor, "SCUBA: a common-user submillimetre camera operating on the James Clerk Maxwell Telescope", Mon. Not. Roy. Astron. Soc., 303, pp. 659—672, 1999.

M. D. King ; W. P. Menzel ; Y. J. Kaufman ; D. Tanre, Cloud and aerosol properties, precipitable water, and profiles of Temperature and water vapor from MODIS, DOI: 10.1109/TGRS.2002.808226, IEEE Transactions on Geoscience and Remote Sensing, 41, 442 – 458, 2003.

Marín J. C., Pozo D., Curé M., A&A, 573, A41, 2015

Pérez-Jórdan G., Castro-Almazán J. A.,Muñoz-Tuñón C., Codina B.,Vernin J., MNRAS, 452, 1992, 2015

Pozo D., Illanes L., Caneo M., Curé M., Rev. Mex. Astron. Astrofis., 41, 55, 2011

Delgado, G.,A., Belitsky, V., & Urbain, D. Otarola, 1999, MMA Memo 271 (NRAO)

D. A. Naylor, I. M. Chapman, B. G. Gom, Measurements of atmospheric water vapor above Mauna Kea using an infrared radiometer, Atmospheric Radiation Measurements and Applications in Climate, Joseph A. Shaw, Editor, Proceedings of SPIE, 4815, 36-45, 2002.

Otárola, D. Hiriart, and J. E. Pérez–León, Statistical Characterization of Precipitable Water Vapor at San Pedro Mártir Sierra in Baja California, Rev. Mex. Astron. Astrofis., 45, 161-169, 2009.

S. J. E. Radford, M. A. Holdaway and J. B. Peterson, Atmospheric transparency at 350μm wavelength, BAAS, 30, pp. 884, 1998.

Tregoning, P., Boers, R., O'Brien, D. and Hendy, M., Accuracy of absolute precipitable water vapor estimates from GPS observations. Journal of Geophysical Research 103. doi: 10.1029/98JD02516. issn: 0148-0227, 1998.

D. D. Turner, S. A. Clough, J. C. Liljegren, E. E. Clothiaux, K. E. Cady-Pereira, and K. L. Gaustad, Retrieving Liquid Water Path and Precipitable Water Vapor From the Atmospheric Radiation Measurement

(ARM) Microwave Radiometers, IEEE Transactions on Geoscience and Remote Sensing, 45, 3680-3690, 2007.

H. Vogelmann and T. Trickl: Wide-range sounding of free-tropospheric water vapor with a differential-absorption lidar (DIAL) at a high-altitude station, Appl. Opt. 47, 2116-2132, 2008.

Acknowledgements

Data of the University of Wyoming archive have been used in the present analysis (weather.uwyo.edu).

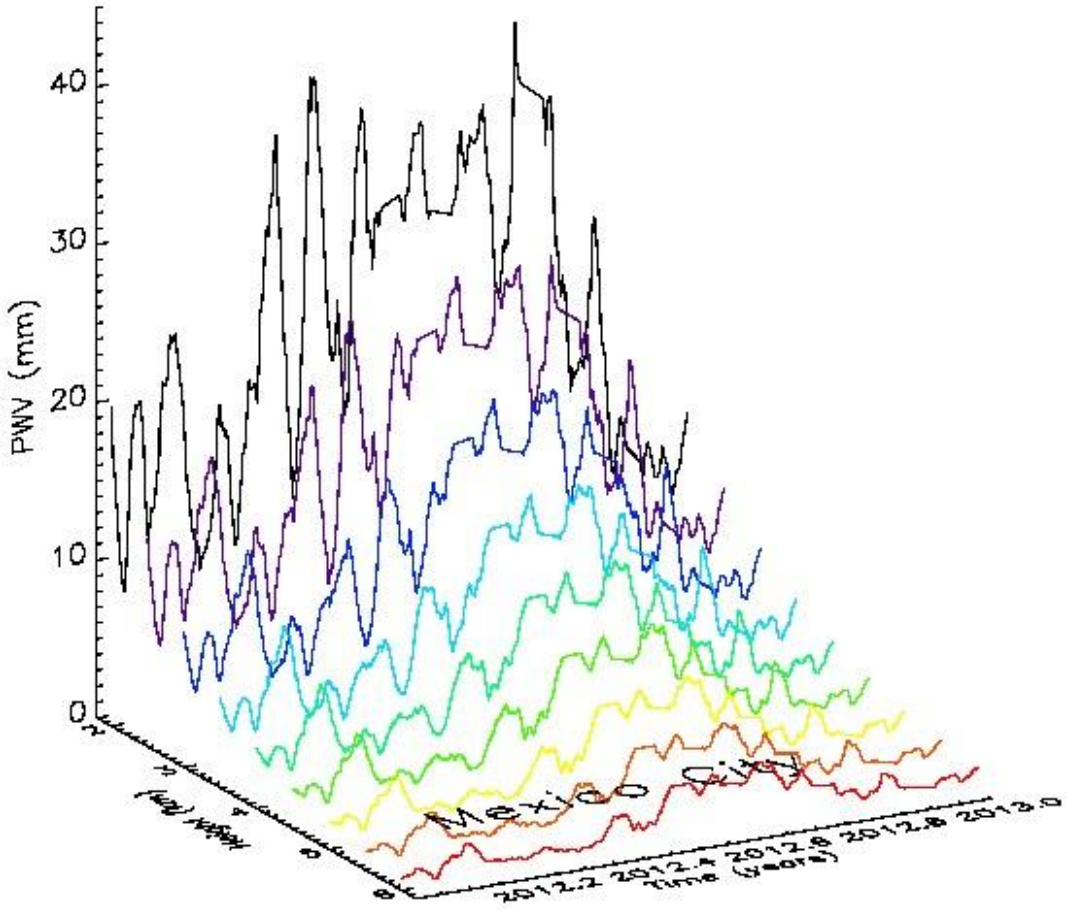

Figure 2. The PWV from January to December 2012, it is integrated from different lower altitudes (black-2 km, violet-2.5 km, dark-blue-3 km, light-blue-3.5 km, dark-green-4 km, light-green-4.5 km, yellow-5 km, orange-5.5 km, red-6 km). In the X-axis the time in years is given, January is at the left hand side and December at the right hand side. In the Y-axis the lower limit of integration is given (from 2.0 to 6.0 km) and in the Z-axis, the PWV (in mm).

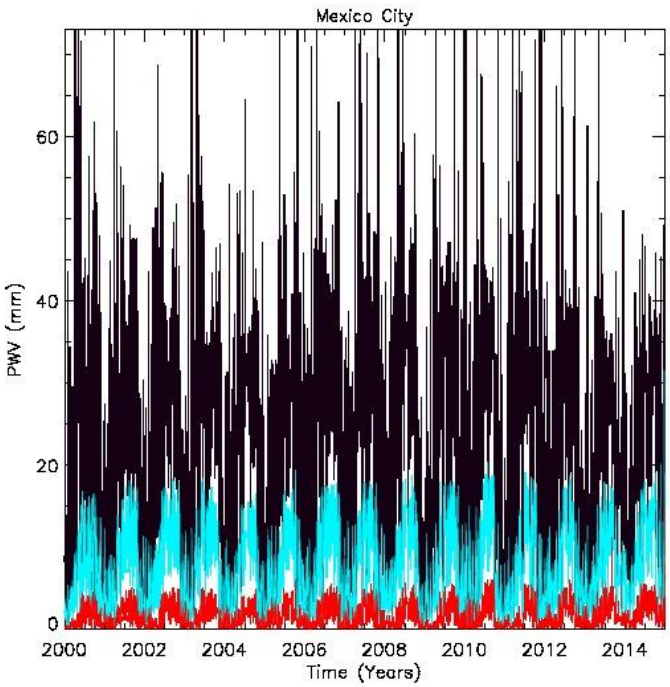

Figure 3. The PWV for a time interval from January 2000 to December 2014, estimated integrating from three different lower altitudes, 2 km (violet), 3.5 km (blue) and 6 km (red).

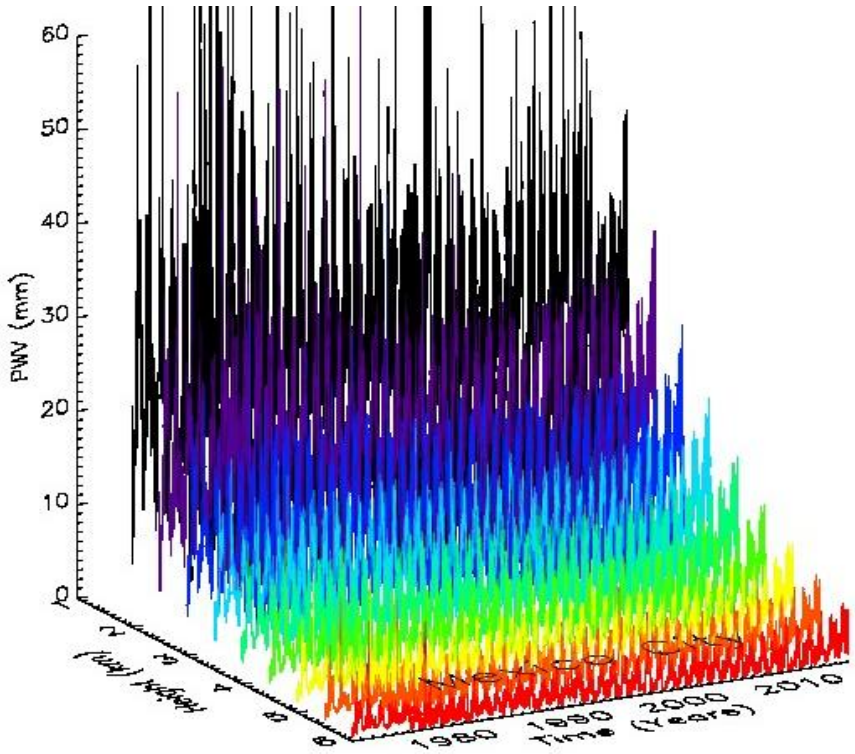

Figure 4. The same as Figure 2, but for the whole period (from 1973 to 2015). The red line represents the PWV integrated from 6 km and the black line, the PWV integrated from 2 km. In the X-axis the time is given, in the Y-axis the lower limit altitude is given and in the Z-axis the PWV.

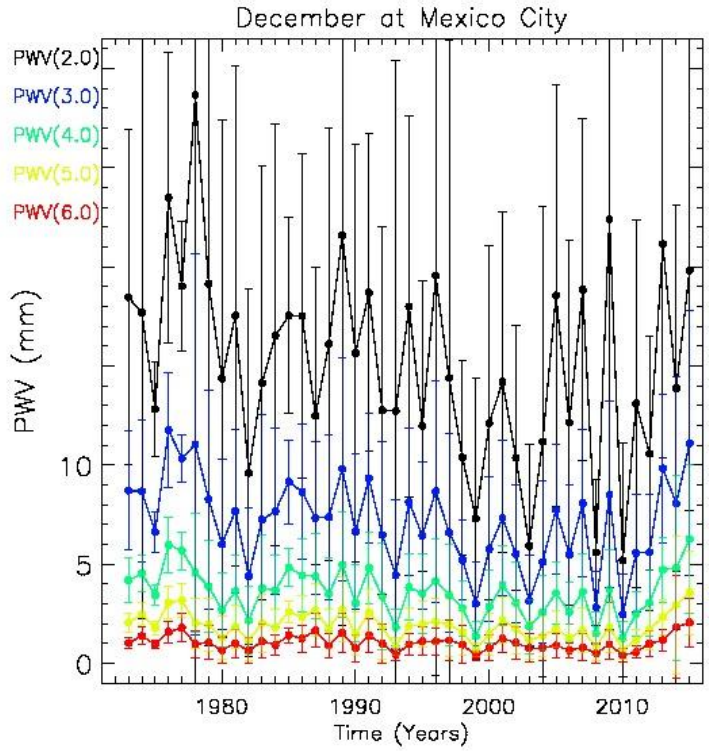

Figure 5. The PWV averaged for each December of each year of the interval 1973-2015 for the lower limits of integration given at the left hand side of the plot. The bars at the average values correspond to the standard deviations, computed for the given month.

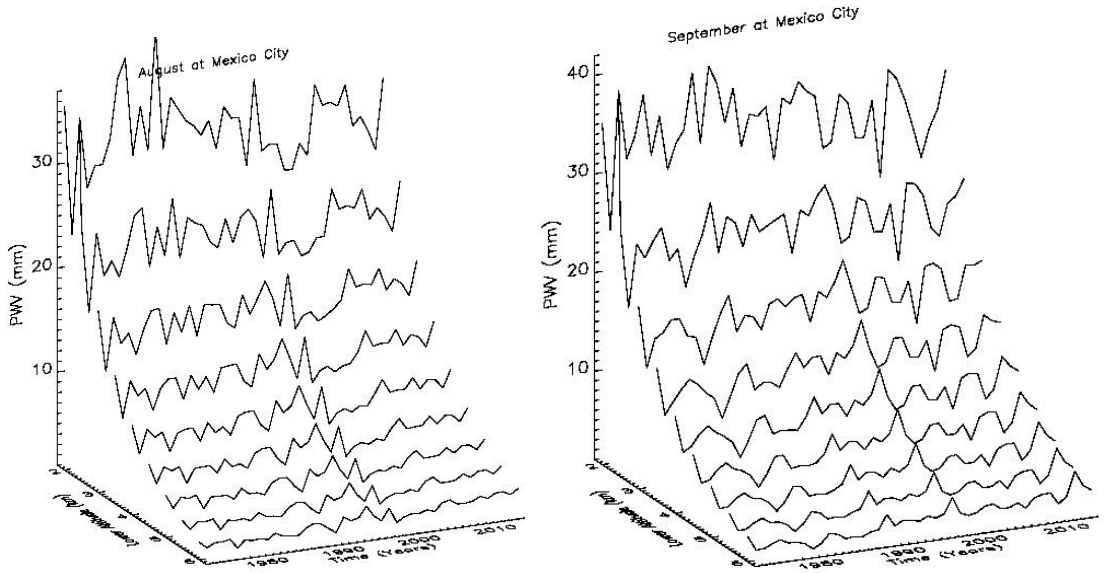

Figure 6. Monthly average of PWV, integrated from the lower limits: 2, 2.5, 3, 3.5, 4, 4.5, 5, 5.5, 6 km (upper to lower curves). The backside curve corresponds to the PWV for 2 km lower limit and the curve at the front side to the PWV for 6 km. In the X-axis the time, in years, is given and in the Y-axis the lower limit of integration, in the Z-axis the PWV is given, **Left** for August of each year of the whole interval and **Right** for September of each year.

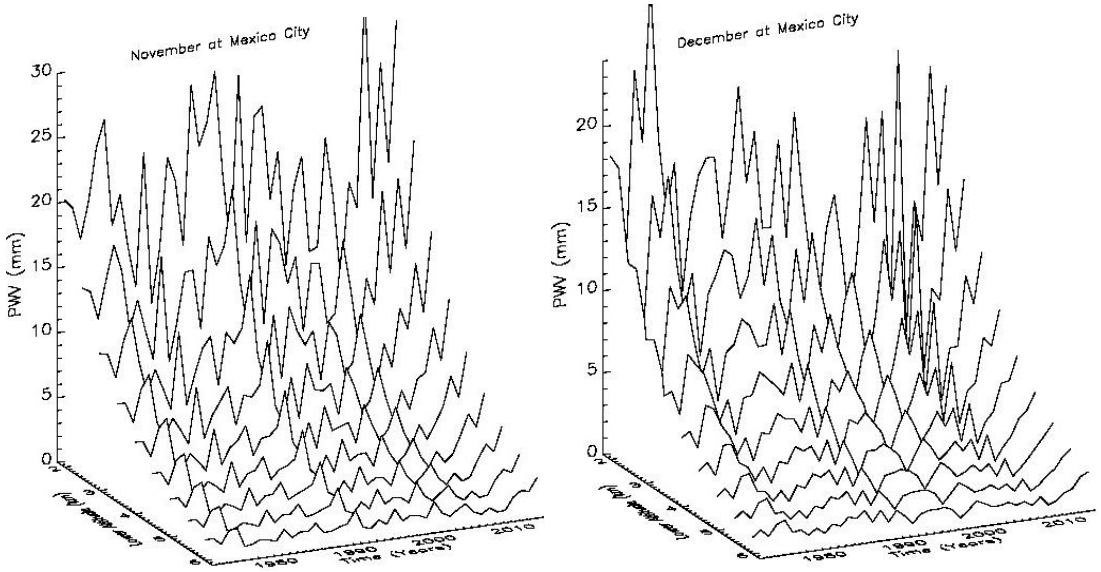

Figure 7. The same as Figure 6, monthly average of PWV, integrated from the same lower limits as Figure 6, **Left** for data of November of each year and **Right** for data of December.

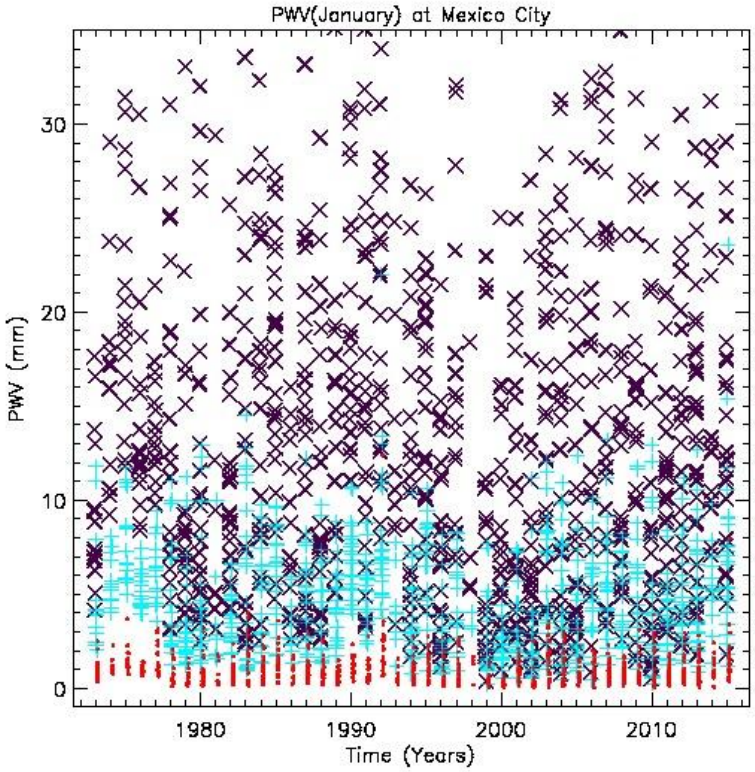

Figure 8. The PWV for all the Januaries of the entire time interval. The red dots correspond to the PWV integrated from the lower altitude of 6 km. The blue crosses correspond to the PWV integrated from 3 km and violet crosses from 2 km.

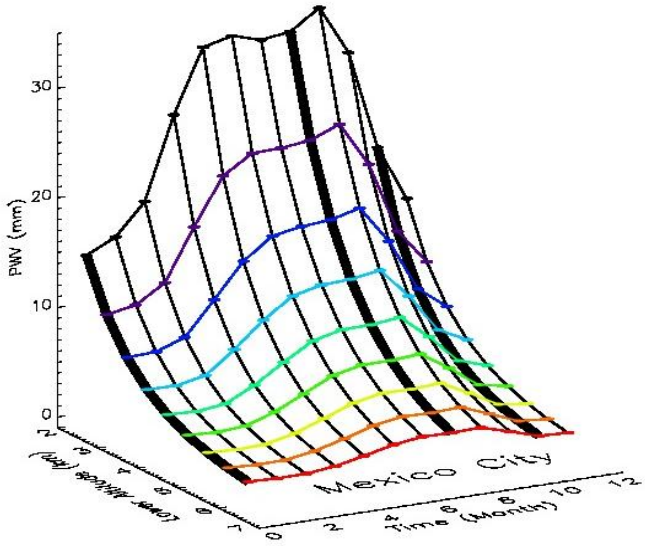

Figure 9. The PWV averaged over all the data of each month, in X-axis the months are given with numbers (1 is for January, 12 is for December), in Y-axis the lower limit of integration is given and in Z-axis the average of PWV (for the data of each month of the entire interval).

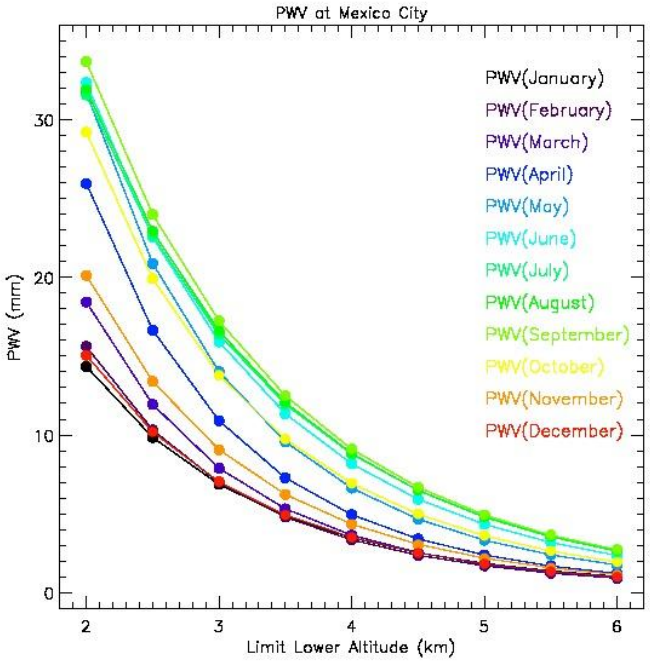

Figure 10. The PWV averaged over all the data of each month. The color, of a given PWV curve, corresponds to the month given in the list at the right of the plot. In the X-axis the lower limit from which the PWV is integrated is given and in the Y-axis the average of the PWV for each month (including all the data of the entire interval). The PWV decays more slowly with altitude at December-February, which means that the scale height is larger at these months.

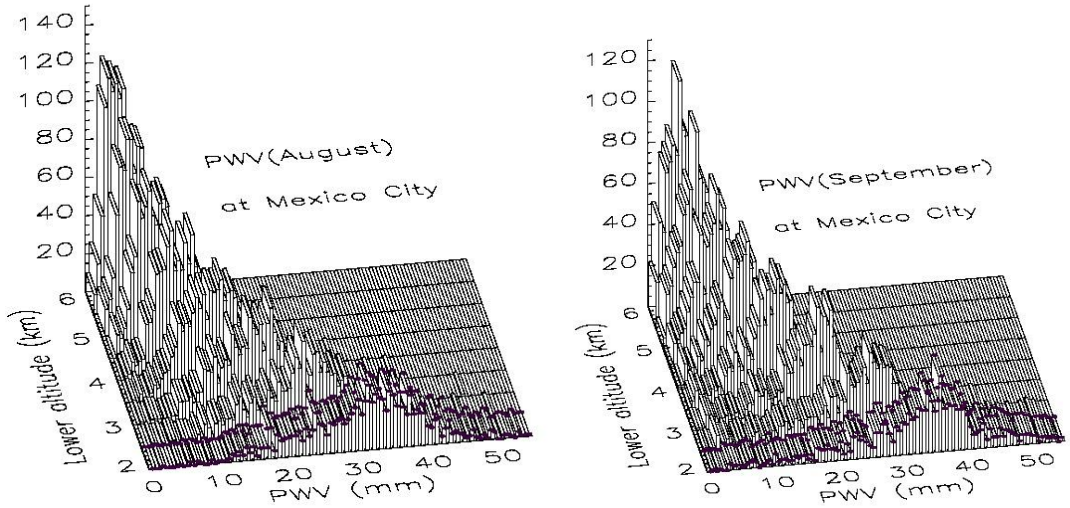

Figure 11. 3D histograms of PWV, in the X-axis the PWV (in mm) is given, in Y-axis the lower altitude (in km) from which the PWV is integrated and in the Z-axis the frequency of occurrence. The histograms are made with data of the entire time interval, from 1973 to 2015, **Left** for all the Augusts of this interval and **Right** for all the Septembers. In this kind of plots the "square mode" suppress the histogram of the back extreme, however those data are seen in Figure 12 in the left extreme (red line).

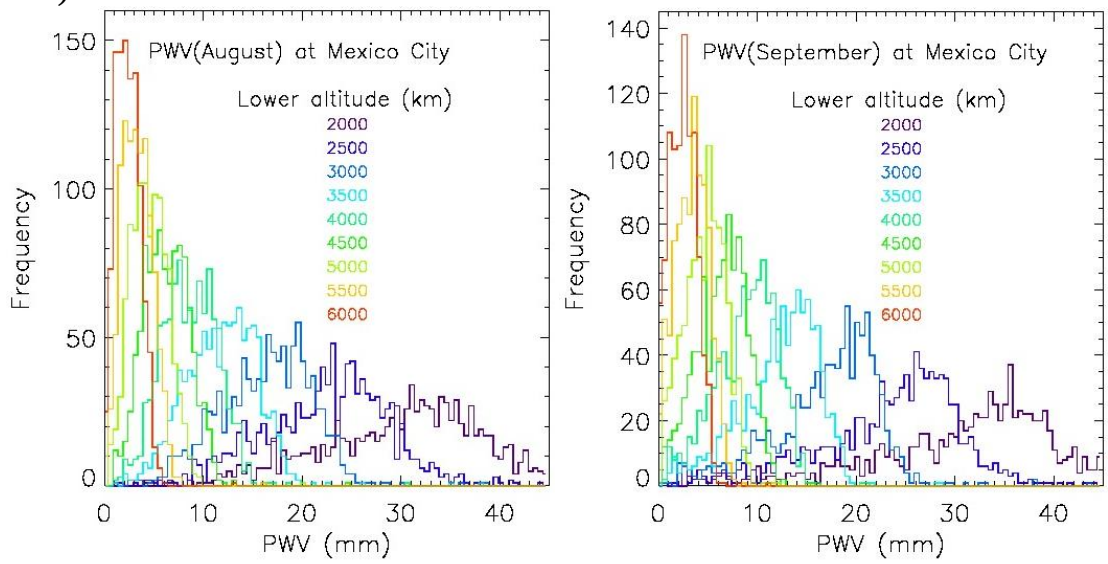

Figure 12. Histograms for PWV estimated from different lower altitudes (given in a list in the center of the plot) for the time interval from 1973 to 2015. The plots are like front views of the plots of Figure 11. It may be seen that the maximum of the histogram shifts to lower values of PWV with the altitude and that the frequency of occurrence around this maximum grows (also with altitude). **Left** Data of all the Augusts and **Right** of all the Septembers of the entire interval.

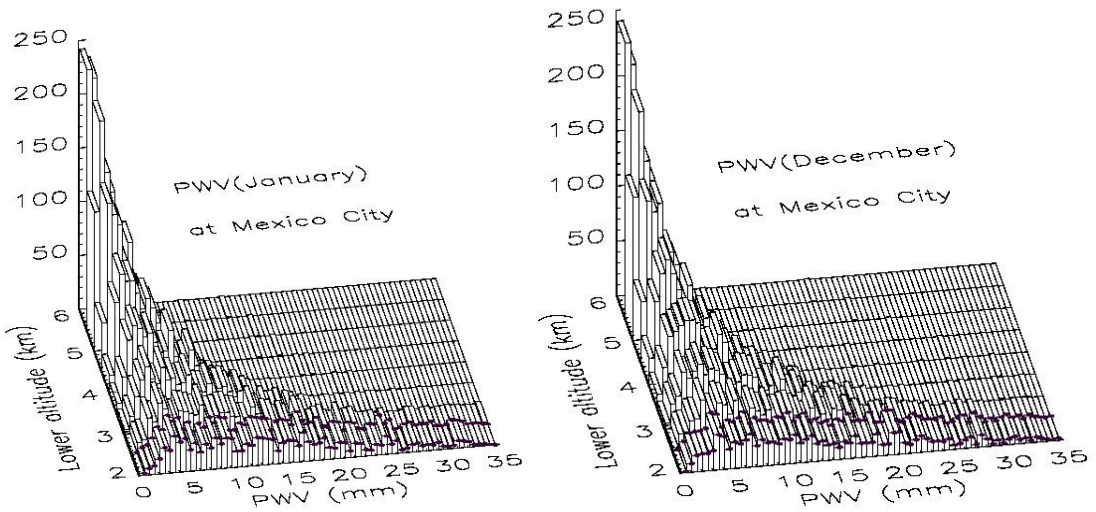

Figure 13. The same as Figure 11, also for data of the time interval from 1973 to 2015, **Left** for the data of all the Januaries and **Right** for all the Decembers of the entire interval.

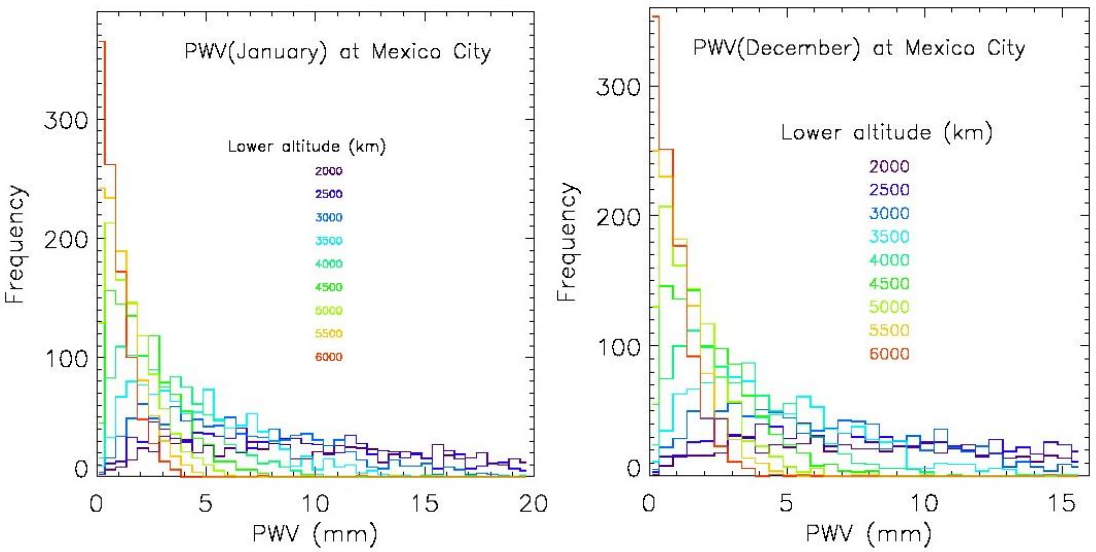

Figure 14. The same as Figure 12, also for the time interval from 1973 to 2015, **Left** for the data of all the Januaries and **Right** for data of all the Decembers of the entire time interval.

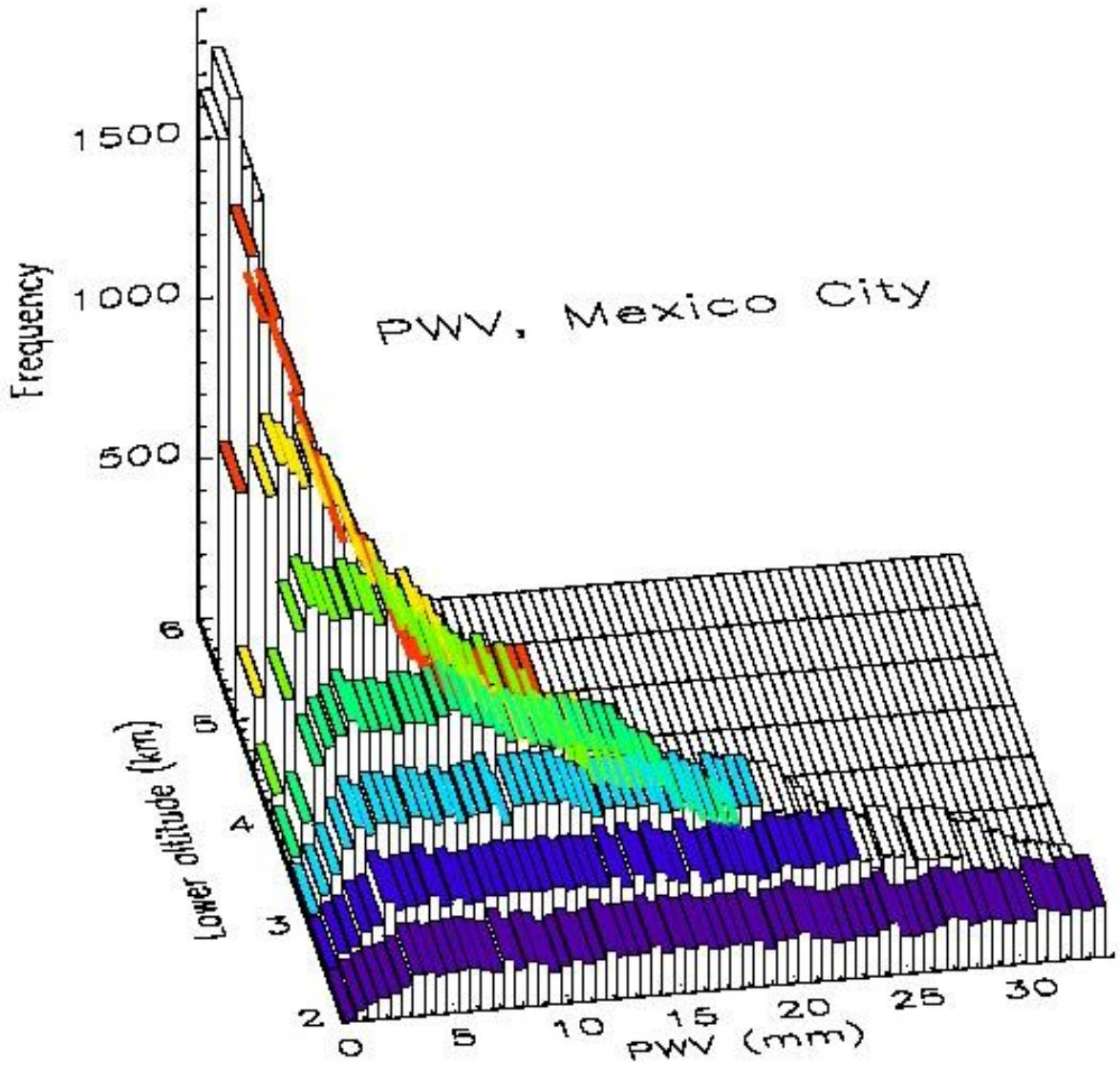

Figure 15. The same as Figure 11, also for data of the time interval from 1973 to 2015, in this case the histogram is for PWV data of all the months.

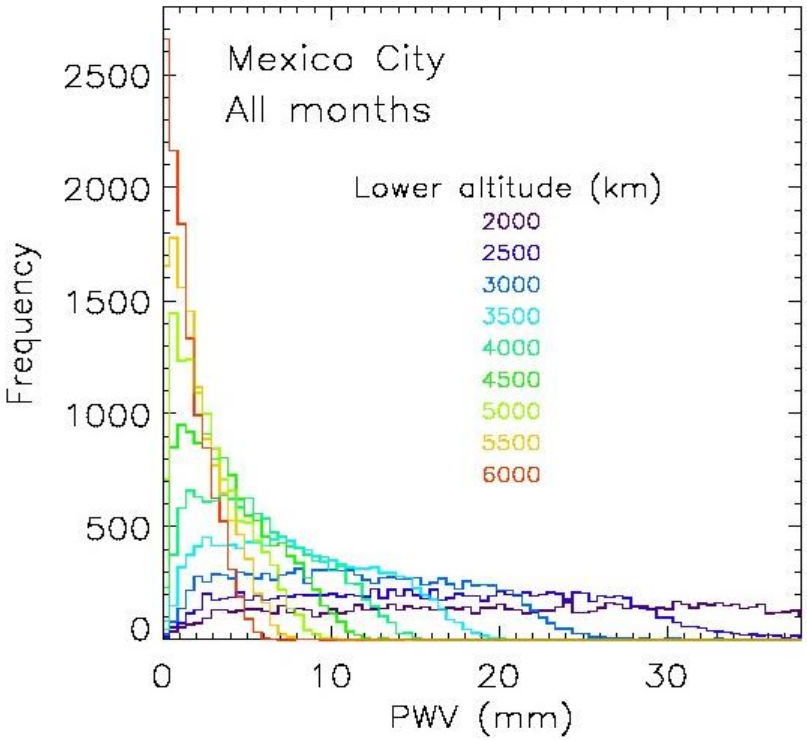

Figure 16. The same as Figure 12, also for the time interval from 1973 to 2015, in this case for PWV data of all the months.

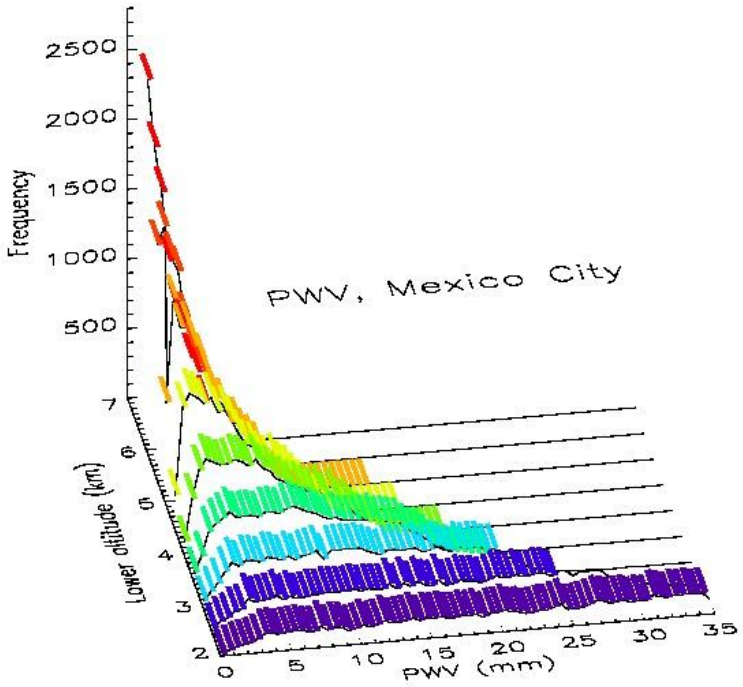

Figure 17. The same as Figure 15, also for the data of all the months. In this case the mode of the plot allows to see the histogram for the higher altitude lower limit (6 km) which is the last on the backside.